Title	Results of x-ray mirror round-robin metrology measurements at the APS, ESRF, and SPring-8 optical metrology laboratories
Author(s)	Assoufid, Lahsen; Rommeveaux, Amparo; Ohashi, Haruhiko et al.
Citation	Proceedings of SPIE - The International Society for Optical Engineering. 2005, 5921, p. 59210J
Version Type	VoR
URL	https://hdl.handle.net/11094/86989
rights	Copyright 2005 Society of Photo-Optical Instrumentation Engineers (SPIE). Downloading of the abstract is permitted for personal use only.
Note	

Results of x-ray mirror round-robin metrology measurements at the APS, ESRF, and SPring-8 optical metrology laboratories

Lahsen Assoufid[1*], Amparo Rommeveaux[2], Haruhiko Ohashi[3], Kazuto Yamauchi[4],
Hidekazu Mimura[4], Jun Qian[1], Olivier Hignette[2], Tetsuya Ishikawa[3,5], Christian Morawe[2]
Albert Macrander[1], Ali Khounsary[1], Shunji Goto[3]

[1]APS, Argonne National Laboratory, 9700 South Cass Avenue, Argonne 60439, Illinois, USA
[2]ESRF, 6 rue Jules Horowitz BP 220, 38043 Grenoble Cedex 9, France
[3]SPring-8/JASRI, 1-1-1 Kouto, Mikazuki-cho, Sayo-gun, Hyogo 679-5198, Japan
[4]Department of Precision Science and Technology, Graduate School of Engineering, Osaka
University, 2-1 Yamada-oka, Suita, Osaka, 565-0871, Japan
[5]SPring-8/RIKEN, 1-1-1 Kouto, Mikazuki-cho, Sayo-gun, Hyogo 679-5148, Japan

ABSTRACT

This paper presents the first series of round-robin metrology measurements of x-ray mirrors organized at the Advanced Photon Source (APS) in the USA, the European Synchrotron Radiation Facility in France, and the Super Photon Ring (SPring-8) (in a collaboration with Osaka University,) in Japan. This work is part of the three institutions' three-way agreement to promote a direct exchange of research information and experience amongst their specialists. The purpose of the metrology round robin is to compare the performance and limitations of the instrumentation used at the optical metrology laboratories of these facilities and to set the basis for establishing guidelines and procedures to accurately perform the measurements. The optics used in the measurements were selected to reflect typical, as well as state of the art, in mirror fabrication. The first series of the round robin measurements focuses on flat and cylindrical mirrors with varying sizes and quality. Three mirrors (two flats and one cylinder) were successively measured using long trace profilers. Although the three facilities' LTPs are of different design, the measurements were found to be in excellent agreement. The maximum discrepancy of the rms slope error values is 0.1 µrad, that of the rms shape error was 3 nm, and they all relate to the measurement of the cylindrical mirror. The next round-robin measurements will deal with elliptical and spherical optics.

Keywords: Long trace profiler, round robin, surface metrology, x-ray mirrors, synchrotron radiation.

1. INTRODUCTION

Most of synchrotron radiation facilities around the world have established dedicated optical metrology laboratories for evaluation and quality control of x-ray mirrors. The main instruments typically used to characterize these mirrors include a microscope interferometer to measure surface roughness, a Fizeau interferometer for figure error measurements, and the long trace profiler (LTP) for surface slope and radius of curvature measurements. The first two instruments are exclusively of commercial nature, while the LTP, originally developed by Takacs *et al.* [1,2], exists in either commercial or in-house-made versions. Because of its ability to provide a direct measurement of the slope and shape profiles of a mirror surface without relying on an external reference optic, the LTP is by far the most used instrument. However, despite its popularity, and except for a limited survey of LTPs published in reference [3] almost a decade ago, no effort has been spent in comparing the performance and accuracy of LTPs and other similar profilers. More specifically, recent advances in mirror-polishing technology and the increasing demand for higher quality optics have stimulated interest in improving existing measurement tools and designing new ones. The goal of these round-robin measurements is to compare LTPs used at the Advanced Photon Source (APS) in the USA, the European Synchrotron Radiation Facility (ESRF) in France, and the Super Photon ring (SPring-8) in Japan. This effort is part of an agreement to promote

*Correspondence: Phone: (630) 252-2774, Fax: (630) 252-9303, E mail: assoufid@aps.anl.gov

exchange of experience and information among experts and specialists at the three facilities. This effort is also joined by Osaka University in Japan as part of their ongoing collaboration with SPring-8 to develop high-quality elliptical Kirkpatrick-Baez (K-B) mirrors for hard x-ray nanofocusing.

The round-robin measurement is divided into two parts. The first part, which is the focus of this paper, deals with LTP measurements of three types of optics: two flats fabricated using two different advanced figuring techniques and one 1-m-long cylindrical mirror with a sagittal radius of 11 cm polished using a conventional technique. The second part of the round robin, to be published at a later date, will focus on the metrology of elliptical K-B mirrors and spherical mirrors. The optics were selected to reflect typical, as well as the state-of-the-art, mirrors used at hard x-ray synchrotron radiation sources. Various LTP parameters and capabilities will be studied including, accuracy, noise level, calibration, etc. Additionally, this collaborative work, along with a similar European round-robin measurement published in these proceedings [4], intends to provide the ground work to assess and understand the limitations of the LTP and other similar profilers, to develop guidelines and procedures to accurately perform measurements with them, and to stimulate research to further improve their accuracy.

2. THE ROUND-ROBIN OPTICS

Optics selected for this first series of round robin measurements include two flat mirrors and one cylindrical mirror. Table 1 summarizes the parameters of the mirrors. One of the flat optics is a 300-mm-long silicon substrate (intended to be used for a multilayer mirror) and was polished using a computer-controlled optical surfacing technique [5]. The second flat mirror, also made of silicon, was 100 mm long and was figured over a 2-mm-wide stripe using a plasma chemical vaporization machining (PCVM) and elastic emission machining (EEM) techniques developed at the Osaka University, Japan [6]. The third mirror is a 1-m-long Pt-coated cylindrical mirror with 11-mm sagittal radius. The two flat mirrors were selected because they exhibit slope and shape errors near, or beyond, the LTP performance limits. In particular, the 100 mm Si substrate was previously measured using microstitching interferometry and showed shape error of 0.4 nm rms [7]. This presents a challenge to the current LTPs. The cylindrical mirror selection was motivated by the fact that the alignment along the LTP scanning direction is critical in performing accurate measurements; a misalignment error can cause the test beam to be reflected off the desired trace and probe a two-dimensional slope instead of the mirror tangential slope alone. Finally, the three mirrors provide measurements over scan lengths that are of short, medium, and long range with a varying degree of surface quality. Each laboratory provided a mount to support the optic during measurement and a detailed written procedure for handling and making measurements. The mirrors' surface roughness values given in Table 1 are average values measured at the three laboratories using interferometer microscopes equipped with 5x objective lenses.

Table 1. Description of the round-robin optics. The surface roughness is the average value of the measurements performed at the three laboratories using roughness interferometer microscopes equipped with 5x objective lenses.

Mirror Owner	APS	ESRF	SPring-8/Osaka University
Material	Silicon	SiO_2	Silicon
Shape	Flat	Toroidal	Flat
Size	$300 \times 40 \times 15 mm^3$	$1000 \times 100 \times 72 mm^3$ Sagittal radius = 11 cm	$100 \times 50 \times 10 mm^3$
Coating	None	Pt	None
rms roughness	2 Å	5 Å	4 Å
Measured length	220 mm	800 mm	70 mm
Manufacturing process	Computer-controlled optical surfacing	Chemical mechanical polishing	Plasma chemical vapor and elastic emission machining

3. LABORATORY ENVIRONMENT

All of facilities' laboratories are housed in a cleanroom environment. Table 2 summarizes their parameters. Additionally, to reduce air turbulence, each LTP is enclosed in a local environment enclosure.

Table 2: Metrology laboratories environment.

	APS	ESRF	SPring-8
Cleanroom type	Cleanroom class 10,000	Cleanroom class 1000	Cleanroom class 10,000
Temperature	21°C±0.1	21°C±0.03	21°C±1
Humidity	50%±10%	50%±10%	50% in summer 30-40% in winter

4. DESCRIPTION OF THE LONG TRACE PROFILERS

The long trace profiler (LTP) is a noncontact slope-angle measuring device that is widely used for measuring the surface figure of synchrotron beamline mirrors. The original LTP designed by Takacs *et al.* [1,2] was based on the pencil-beam interferometer technique originally developed by Von Bieren [8]. Literature describing the principle of an LTP is abundant, and over the years many variations have been designed and operated worldwide. Briefly, the LTP optical arrangement is designed to produce a probe beam with two components spaced with an adjustable distance, d. The two beam components form a zero-optical-path difference interferometer with an infinite depth of field. Upon reflection from the surface under test (SUT), they carry the information on the local slope and are directed by a polarizing beam splitter to a Fourier transform (FT) lens. The FT lens focuses the two beams onto a linear array detector to produce an intensity pattern that has a minimum surrounded by two peaks. As the surface slope changes, the minimum of the intensity pattern translates across the linear array detector. The location of this minimum is directly proportional to the local surface slope. The laser source is typically a He-Ne stabilized laser with the beam channeled to the optics board via a polarization-preserving fiber optic link. In a typical LTP system, the optics board is mounted on a linear air-bearing slide that allows one to scan a long mirror and obtain a one-dimensional slope profile of its surface. The whole assembly is mounted on a vibration-isolation table. The commercial version of the LTP was developed during late 1980s in a collaboration between Brookhaven National Laboratory, Lawrence Berkley National Laboratory, Continental Optical Corporation, and Baker Engineering [9].

The APS's long trace profiler (Figure 1), APS LTP II, is the second generation of its kind and was commissioned in 1994. The system incorporates a number of improvements including an internally generated reference beam that is used to correct for tilt errors of the optical board; a dove prism is incorporated into this reference beam to correct for phasing problems between the mechanical and thermal errors; and there is an environment enclosure that stabilizes the temperature to within ±0.1ºC, which greatly improved the instrument repeatability [10]. The system has an angular range of ±5 mrad and can handle mirrors up to two meters long.

The ESRF's LTP (Figure 2) is an evolving version of the original design by Takacs *et al.* [1,2]. It was built in 1993 but has undergone many upgrades [11-12]. However, here part of the optics board and the detector are stationary, and a moving pentaprism assembly directs the test beam onto the surface to be scanned. This design is equivalent to the pentaprism LTP developed by S. Qian *et al.* [13], except that a mirror arrangement is used to construct an equivalent of a pentaprism. As a result, systematic measurement errors due to possible glass inhomogeneity in commercial standard pentaprisms can be avoided. The main advantage of this LTP design is that no compensation is needed for errors due to the moving pentaprism carriage. The main disadvantage is the continuous increase of the optical path length of the laser test beam as the mirror is being scanned from one end to the other, which makes the instrument sensitive to environment perturbations. To reduce the effects of environment perturbations, the instrument is enclosed in a Plexiglas enclosure and

a reference beam reflected from a fixed mirror provides a signal to correct for environment-induced instabilities inside this enclosure. The system has an angular range of ±6 mrad and can measure mirrors up to 1.5 meters long.
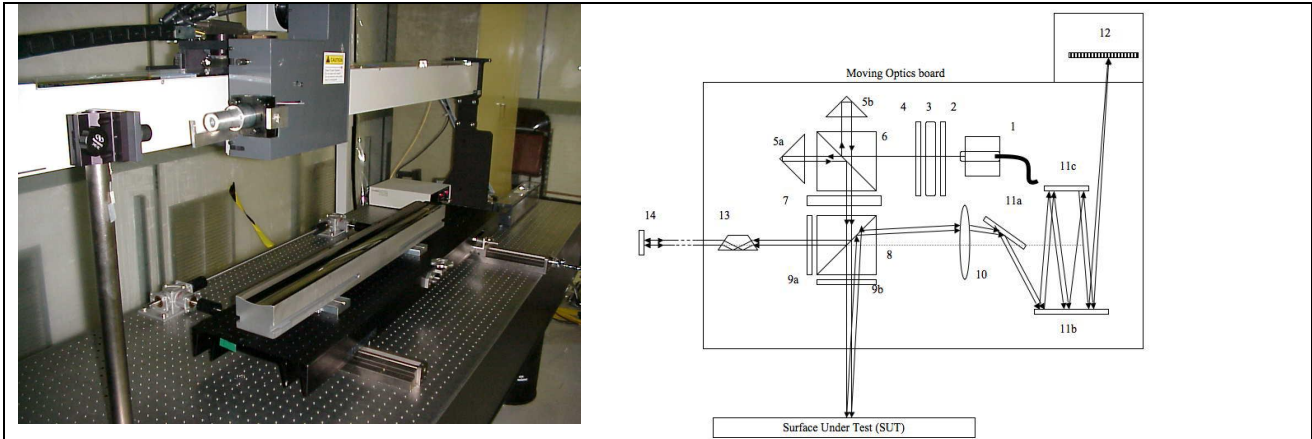

Figure 1: Photograph of the APS LTP II (left) and a schematic depicting its optics board where 1 = laser fiber mount, 2 = fixed polarizer, 3 = rotating polarizer, 4 = fixed polarizer, 5a&b = porro prisms; 6 = beam splitter, 7 = rotating half-wave plate, 8 = polarizing beam splitter, 9a&b = quarter-wave plates, 10 = Fourier transform lens, 11a-c = folding mirrors, 12 = 1024-pixel double-array detector, 13 = dove prism, 14 = stationary reference mirror.
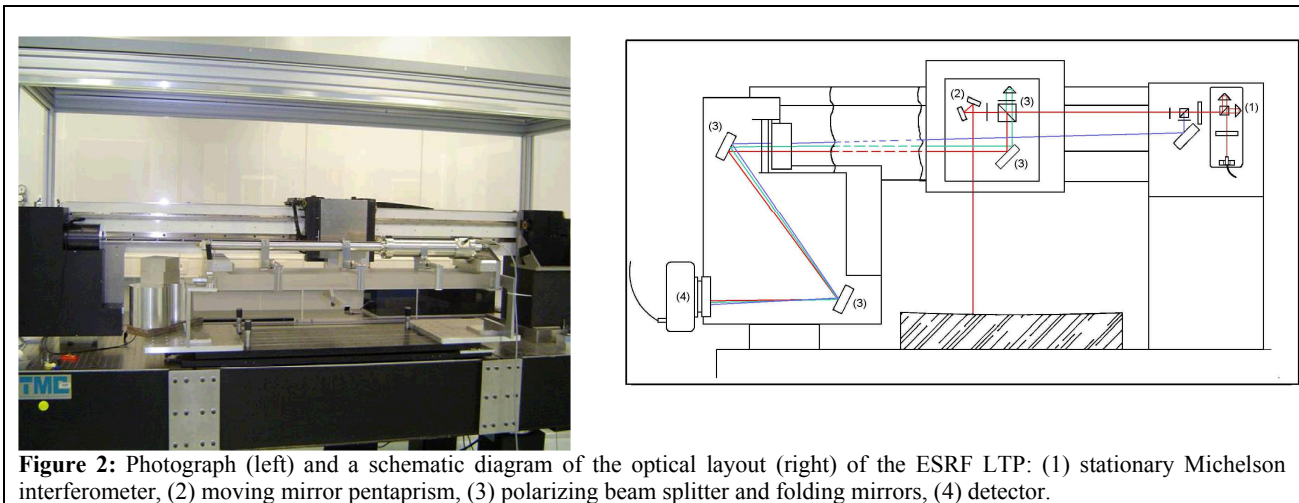
Figure 2: Photograph (left) and a schematic diagram of the optical layout (right) of the ESRF LTP: (1) stationary Michelson interferometer, (2) moving mirror pentaprism, (3) polarizing beam splitter and folding mirrors, (4) detector.

The SPring-8 LTP (Figure 3) is basically a standard LTP II and was acquired in 1999; the basic components (optics board, detector, and motor drive system) are similar to those of the APS LTP II. However, it is of a pentaprism configuration (see Figure 3) [13]. The optics board is fixed on a stationary pedestal, and a small, lightweight pentaprism mounted on an air bearing carriage is translated along a 1.5-meter-long ceramic to direct the test beam to, and scan, the mirror surface. Mirrors up to 1 meter in length can be measured in either upward or sideways configurations. For the latter, the LTP is set up so that the entire optics board is rotated by 90 degrees about the laser beam optical axis, and the two components of the probe beam are oriented in the horizontal plane. The system has two different optics boards, one has an angular measurement range of ±5 mrad, and an optional board can be used to increase the measurable angular range of up to ±30 mrad.

The LTPs at the APS and SPring-8 use the data acquisition and processing software written by Takacs *et al.* [1,2], and the ESRF LTP uses in-house developed software. For each scan, the acquired intensity profile is stored in the system computer hard disc. In the case of the APS and SPring-8 LTPs, the intensity-to-slope conversion is performed on the stored intensity data files by a least squares curve fitting (LSF) algorithm that locates the pixel position of the minimum

in the double-peaked intensity pattern. The LSF used in the pixel-to-slope conversion fits a second-order polynomial function to each intensity pattern stored in the raw intensity data file. For the ESRF LTP, the fast Fourier transform method is used to locate the minimum and convert the stored intensity data into slope data.

One of the main ESRF LTP features is its ability to scan an optic on the fly at a speed of 40 mm/sec, thus providing a smooth mirror scan and fast data acquisition, while the APS and SPring-8 LTP make a stop at each measurement point and the average measurement speed is only 2 mm/sec. Another difference of the ESRF LTP resides in its 1024-pixel, single photodiode detector, which allows slope data to be collected in a single scan (i.e., with no averaging) with a very low noise level. Both the APS and Spring-8 LTPs have a double 1024-pixel photodiode array detector, one array is designated to collect the reference signal, while the other is reserved for the probe beam signal; however, data from a single scan is generally noisier than for the ESRF LTP, and, therefore, multiple-scan averaging is required to reduce random errors. Table 3 summarizes the features of the three instruments.

To reduce the effects of air turbulence, all of the LTPs are housed inside a local environment enclosure.
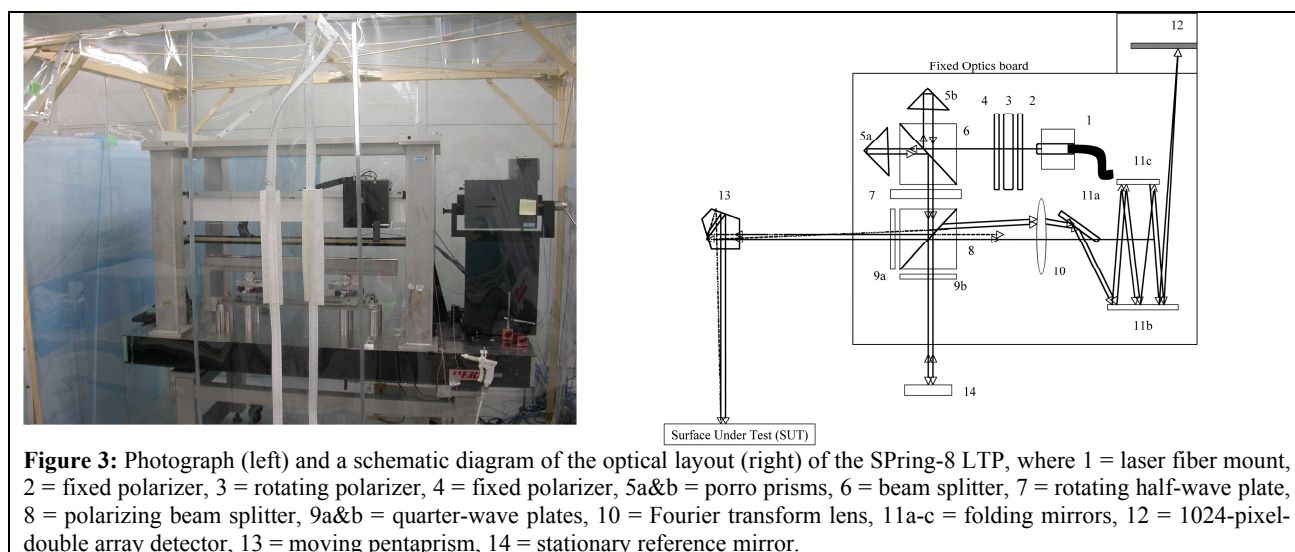

Figure 3: Photograph (left) and a schematic diagram of the optical layout (right) of the SPring-8 LTP, where 1 = laser fiber mount, 2 = fixed polarizer, 3 = rotating polarizer, 4 = fixed polarizer, 5a&b = porro prisms, 6 = beam splitter, 7 = rotating half-wave plate, 8 = polarizing beam splitter, 9a&b = quarter-wave plates, 10 = Fourier transform lens, 11a-c = folding mirrors, 12 = 1024-pixel-double array detector, 13 = moving pentaprism, 14 = stationary reference mirror.

Table 3: Summary of the long trace profiler's features.

	APS (USA)	ESRF (France)	SPring-8 (Japan)
Instrument type	Commercial LTP	In-house-made LTP	Commercial LTP
Instrument operating since	1994	1994	1999
Type of scanning/Measurement speed	Moving optics board/ Point by point @ 2 mm/sec	Moving pentaprism/ On the fly @ 40 mm/sec	Moving pentaprism/ Point by point @ 2 mm/sec
Laser source	Stabilized HeNe Laser @ λ=632 nm	Stabilized HeNe Laser @ λ=632 nm	Stabilized HeNe Laser @ λ=632 nm
Maximum scan length	2 m	1.5 m	1 m
Detector	Dual 1024 pixel array	1024 pixel array	Dual 1024 pixel array
Pixel size	25 μm x 2.5 mm	25.4 μm x 0.5 mm	25 μm x 2.5mm
Spatial sampling	1 mm	1 mm	1 mm
Maximum angular range	±5 mrad	±6 mrad	±5 and ±30 mrad
rms of the difference of 2 successive scans	0.5 μrad	<0.5 μrad	0.5μrad
Slope error rms repeatability	0.1 μrad	≤0.02 μrad	0.1μrad

5 MEASUREMENTS, DATA ANALYSIS, AND RESULTS

5.1 Mirror setup

All of the optics used in this work were measured facing up, i.e., the probe beams are vertically descending on the test mirror surface. The mirrors were scanned along their longitudinal axis over a well-defined trace length. The sampling distance was 1 mm. To minimize errors due to mounting and setup, each owner provided a kinematic mount that was shipped with the mirror. The mounts for the two flat mirrors consisted of three stainless steel (SS) ball bearings spaced by L/2, approximately the Bessel points (0.559L), in the longitudinal direction and centered on the mirror transverse axis, while the cylindrical support points consisted of two10-mm-diam SS rods spaced with the same distance of L/2 around the mirrors transverse axis. Here L is the length of the mirror. This spacing distance minimizes deflection due to gravity, and the use of the same mounting hardware facilitates measurement.

5.2 Measurement procedure

After the setup was completed, the mirrors typically took form one to several hours to reach temperature equilibrium before initiating the measurements. It was agreed that each mirror be scanned and then rotated 180º around the vertical axis and scanned again, and the LTP operator had to ensure that scans of the two orientations were performed along the same trace on the mirror surface. Additionally, to reduce random-noise errors, ten scans were taken at each orientation and the results were averaged. The data of the 180-degree orientation was numerically flipped by 180 degrees before it was averaged with zero-degree orientation data to obtain the final mirror slope profile. This reduces symmetric systematic errors [14].

5.3 Data detrending and slope and shape error calculation

After raw intensity data were converted to slope data, the next step was to remove the reference profile and to detrend the data. The detrending process consisted of removing a least square fit polynomial from the original slope data. Detrend0 removes a constant from the data and detrend1 (i.e., a line fit to slope data) removes the best-fit cylinder from the detrend0 data and therefore gives the slope error profile. The shape error profile was obtained by first converting the detrend0 slope profile into a height profile, then subtracting the best-fit second-order polynomial from the resulting height data. To minimize numerical errors, all the measurements were processed using the same computer program.

5.4 Power spectral density profile calculation

One of the most used parameters for comparing measurements of instruments having different bandwidths is the power spectral density (PSD) function. This material is covered in many publications and will not be discussed here in detail. A computer code, based on the algorithm by Church and Takacs [15], was written and used to calculate the PSD profile from the shape error profile. For a discrete profile, the PSD is typically calculated using the fast Fourier transform algorithm and is described by the following equations:

$$S(f_m) = \frac{2D}{N}|FFT|^2 K(j) \qquad (1)$$

$$FFT = \sum_{n=1}^{N} e^{i2\pi(n-1)(m-1)/N}W(n)zD(n), \qquad (2)$$

where *FFT* is the discrete Fourier transform, $f_m=(m-1)/ND$ is the spatial frequency, *m=1* to *N/2+1* is frequency index (*m=1* corresponds to f_m=0 and gives the profile DC component), *W(n)* is the data window, $zD(n)$ is the detrended data, and *K(j)* is a bookkeeping factor and is equal to 1 for all values of *j* except *j*=1 and *j=1+N/2*, where it is equal to 0.5. The detrended data, $zD(n)$, is the shape error profile obtained by fitting the raw height data to a second-order polynomial. The data window function, $W(n)$, is used to smooth out the ends of the profiles and eliminate spurious effects. We used the Blackman window function recommended for surface profile data [15]:

$$W(n) = \sqrt{\frac{2}{1523}} \left[21 - 25\cos(2\pi(n-1)/N) + 4\cos(4\pi(n-1)/N) \right]. \tag{3}$$

5.5 Measurements and results of the 1-m-long cylindrical mirror

Figure 1 shows a photograph of the mirror mounted under the APS LTP II. The mirror was used to focus a monochromatic beam in the ESRF insertion device (ID 21) beamline. As mentioned in section 1, the challenge in accurately measuring a cylindrical mirror is the alignment of the mirror's longitudinal axis with the LTP scanning direction. Moreover, the tight sagittal radius of curvature causes the probe beams to be defocused in the transverse direction. However, this does not significantly affect the fringe pattern in the scan direction, and, therefore, no corrective cylindrical lens was used to refocus the probe beams.

Figures 4 and 5 show the slope and shape error profiles, respectively. Both profiles are displayed overlapped (right plots) and shifted relative to each other (left plots) for easy comparison. Statistical data are summarized in Table 4. The three measurements are in remarkable agreement. The profiles exhibit nearly identical features with the maximum discrepancy of rms values of only 0.1 µrad for the slope error profiles and 3 nm for the shape error profiles. Both the APS and SPring-8 slope error profiles exhibit high-frequency components, while the ESRF slope error profile is relatively smooth. The fine details of the ESRF and APS profiles are overall nearly identical. Figure 6 shows the PSD profiles derived from the shape error data. The three PSDs of the unfiltered data (Figure 6 left) diverge at the high-frequency end starting at about 6 mm^{-1} with the SPring-8 PSD showing stronger high-frequency components, while the ESRF PSD exhibits a rapid fall off. The PSD profiles computed from smoothed data (see Figure 6 right) show very good agreement, except at the spatial period range from approximately 11 mm up to 18 mm, where the SPring-8 PSD profile has lower power. The smoothing is obtained by applying a 7-point box filter to the residual shape data. This does not reflect the actual frequency cut-off of each instrument. Moreover, it is obvious that the filtering process causes a loss of information about the mirror profile. A further detailed study is needed to determine the actual frequency cut off. Finally, the radii of curvature reasonably agree. The discrepancy could result from the inconsistency of the mirror mounting, environment perturbations, or simply a lack of calibration. The radius of curvature measurement will be the subject of the next round-robin measurements.

Table 4: Results of the 1-m-long cylindrical mirror measurements.

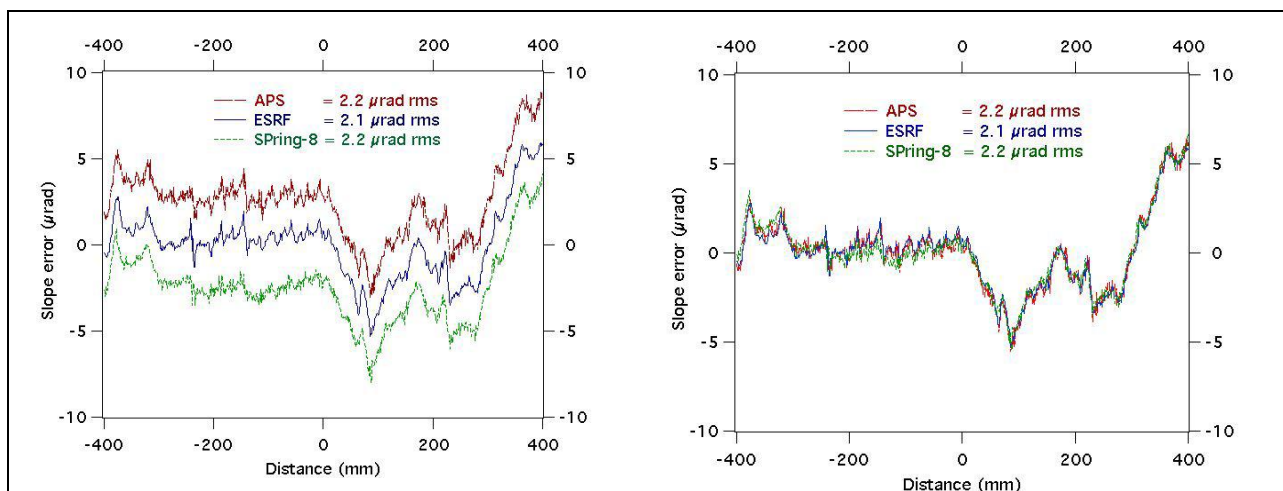| LTP measurements @	Slope error (µrad)	Shape error (nm)	Radius (km)
APS	2.2	94	12.9
ESRF	2.1	91	12.1
SPring-8	2.2	92	12.4

Figure 4: Results of the cylindrical mirror measurements: slope error profiles shifted for clarity (left) and overlapped (right).
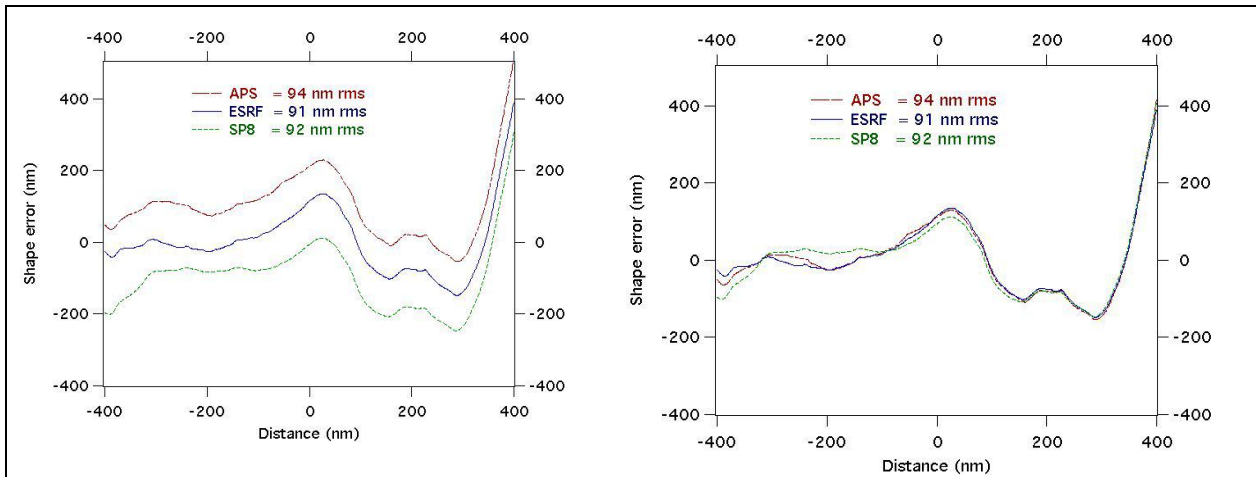

Figure 5: Results of the cylindrical mirror measurements: shape error profiles shifted for clarity (left) and overlapped (right).
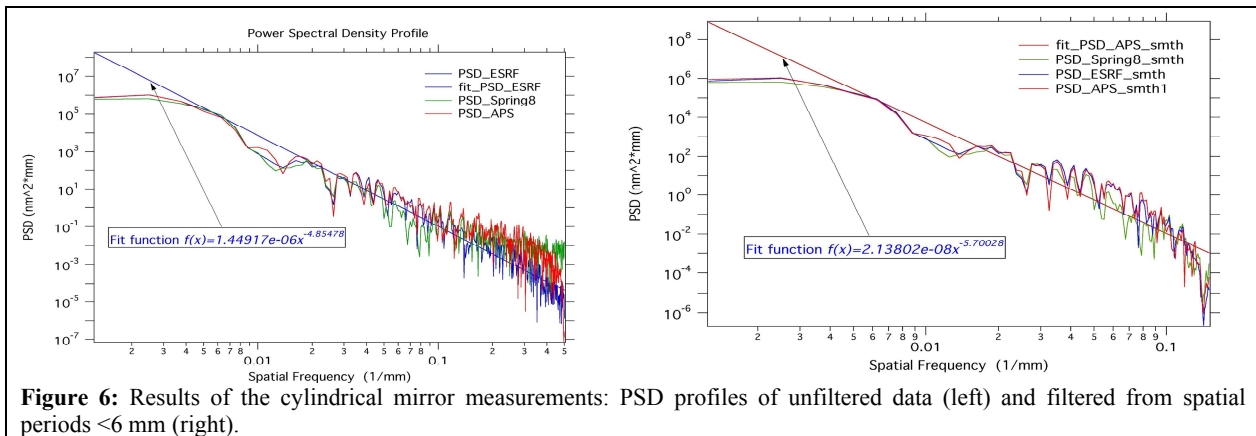

Figure 6: Results of the cylindrical mirror measurements: PSD profiles of unfiltered data (left) and filtered from spatial periods <6 mm (right).

5.6 Measurements and results of the 300 mm Si substrate

This mirror was fabricated using a proprietary computer-controlled optical surfacing technique [5]. The useful aperture is 240 mm, but the measurements were limited to a 220 mm central length along the mirror longitudinal axis. Table 5 summarizes the LTP results. Figure 7 shows plots of the slope error (left) and shape error (right) profiles. For clarity and easy comparison, the slope error profiles were deliberately shifted by a constant along the vertical coordinate. The profiles exhibit many similarities, and their statistical data are in a close agreement. The maximum difference of rms values was 0.05 µrad for the slope error and 0.3 nm for the shape error. Moreover, the shape error profiles all showed the same fabrication artifact at the center of the mirror. The PSD profiles are displayed in Figure 8. Similar to the cylindrical mirror, the PSD profiles show a better agreement when the data is filtered (Figure 8, right) using a 7-point box filter; however, some discrepancy remains at the low-frequency range within 10-50 mm periods.

Table 5: Results of the 300 mm Si substrate measurements.

LTP Measurements @	Slope error (µrad)	Shape error (nm)	Radius (km)
APS	0.36	4.7	41.9
ESRF	0.29	4.5	47.4

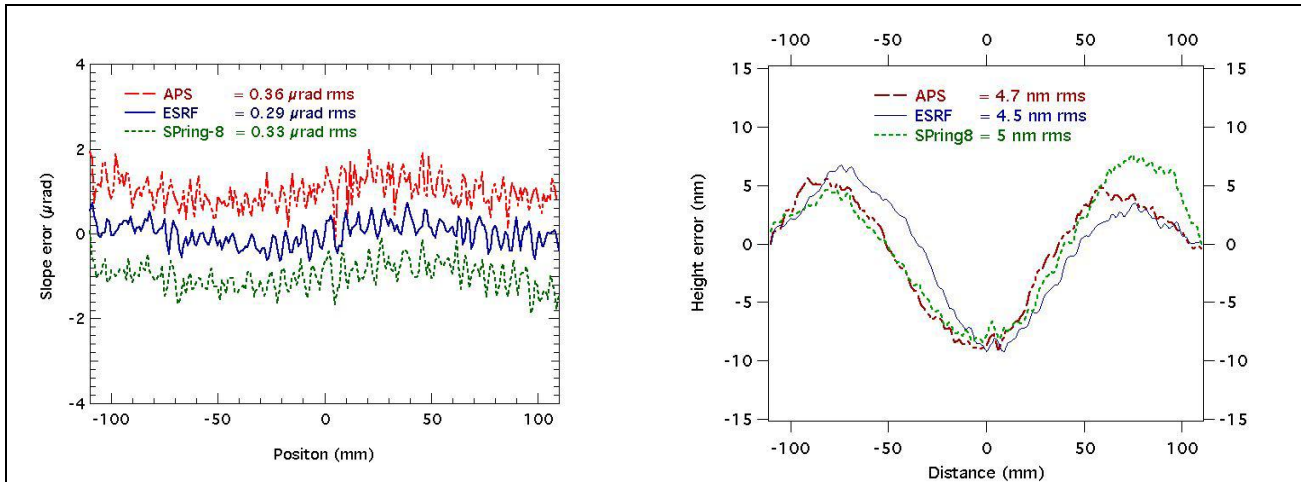| SPring-8	0.33	5	77.9

Figure 7: Results of the 300 mm Si substrate measurements: Slope error profile (left) and shape error (right). For clarity, the slope error profiles are shifted relative to each. Note the common feature displayed by three all of the LTPs shape profiles; this indicates the consistency of measurements.
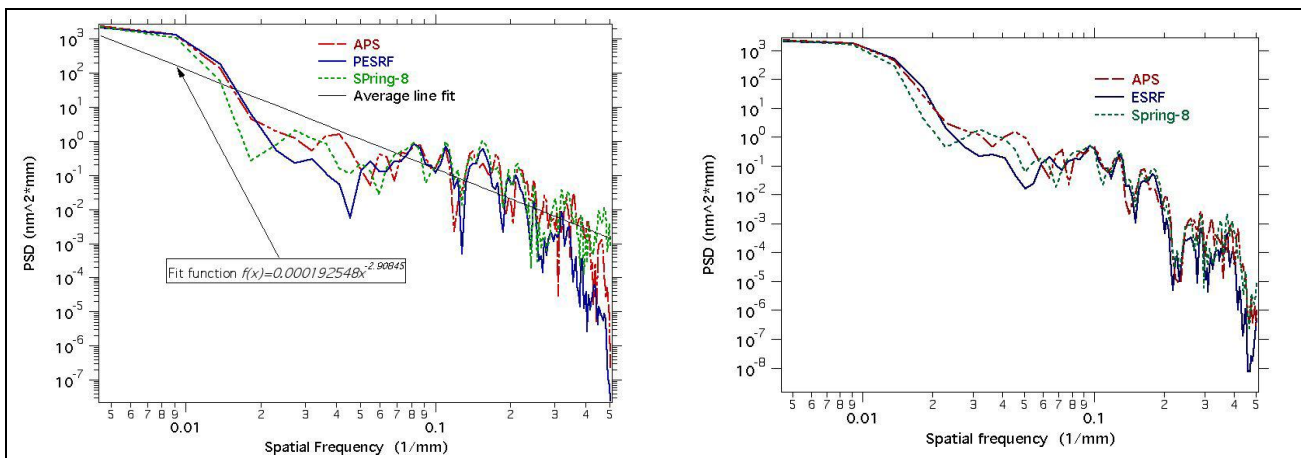

Figure 8: Results of the 300 mm Si substrate measurements: PSD profiles of unfiltered data (left) and filtered from spatial periods <6 mm (right).

5.7 Measurements and results of the 100 mm Si substrate

As mentioned in section 2, the substrate was figured over a narrow strip, 2 mm wide, using plasma chemical vapor machining and elastic emission machining developed at Osaka University [6]. The mirror was previously evaluated using microstitching interferometry and showed a shape error of 0.4 nm rms over the spatial frequency range of 0.2 mm to 70 mm, which probes spatial periods beyond the LTP capability.

Table 6 summarizes the measurement results. Figure 9 compares LTPs original (left) and smoothed (right) slope error profiles with the microstitched slope profile calculated by differentiating the microstitched shape error data. The noise-to-signal ratio of the LTP slope error data appear to be quite significant but the four curves show similar trends. Note that the microstitched data sampling distance was 0.1 mm and, therefore, covers a much wider spectrum than the LTPs, which have a sampling distance of 1 mm. For clarity, the microstitched slope error profile was smoothed by filtering out high-frequency components from the original data. Figure 10 compares LTPs shape error profiles with the microstitched shape error data. Although, the mirror figure error is beyond the limit of standard LTP resolution, the shape error profiles derived from LTPs measurements are consistent and agree well with the microstitched data. Note that the rms height

values for the microstitched profile is from unfiltered data. It is understood that the proper practice to compare profiles that cover unequal bandwidths is to calculate the rms value from integration of the power density profiles over identical bandwidths. Figure 11 shows the PSD profiles derived for the smoothed shape error profiles. The four profiles follow approximately the same slope trend with the PSD from the stitched data rising, as expected, at the high-frequency end. However, the four PSD profiles differ considerably in their fine details. This is not surprising considering the high quality of the mirror. The large discrepancy in the radii of curvatures is also to be expected because the optic is nearly flat and, in this case, computing the radius by fitting noisy data is prone to errors. However, the three LTPs all agree on the sign of the mirror curvature, which is slightly convex.

Table 6: Results of the 100 mm Si substrate measurements derived from filtered LTP data.

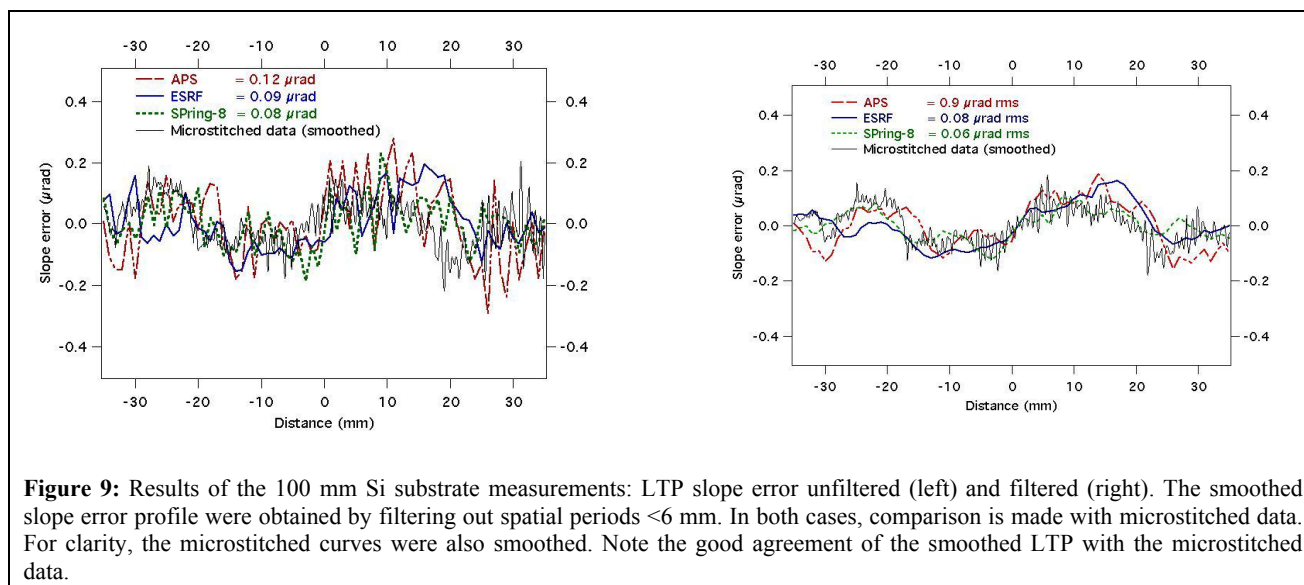| LTP measurements @	Slope error (µrad)	Shape error (nm)	Radius (km)
APS	0.09	0.4	-63
ESRF	0.08	0.4	-139
SPring-8	0.06	0.3	-29

Figure 9: Results of the 100 mm Si substrate measurements: LTP slope error unfiltered (left) and filtered (right). The smoothed slope error profile were obtained by filtering out spatial periods <6 mm. In both cases, comparison is made with microstitched data. For clarity, the microstitched curves were also smoothed. Note the good agreement of the smoothed LTP with the microstitched data.
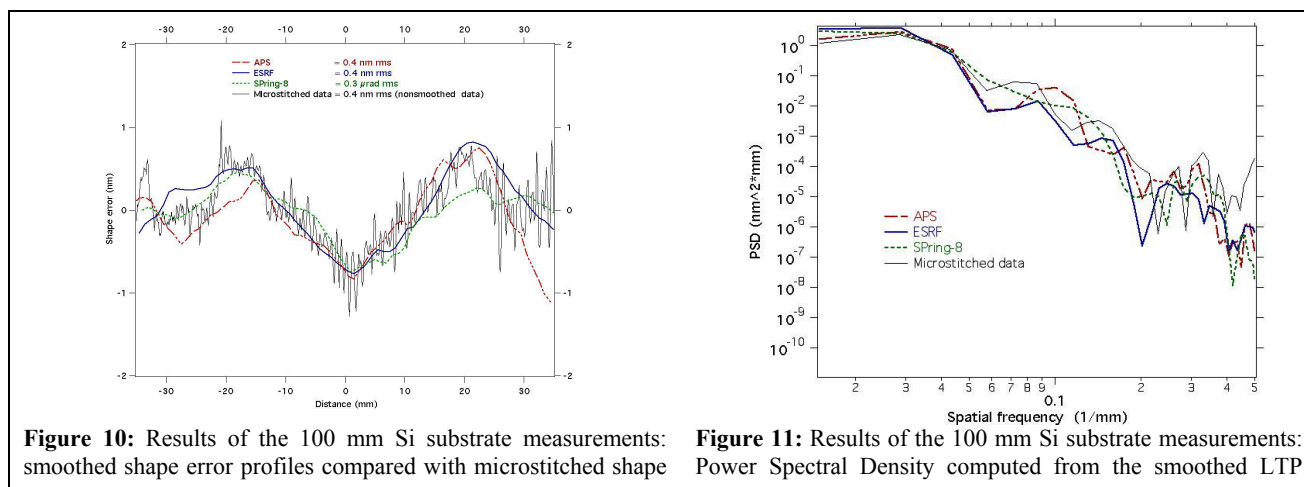

Figure 10: Results of the 100 mm Si substrate measurements: smoothed shape error profiles compared with microstitched shape
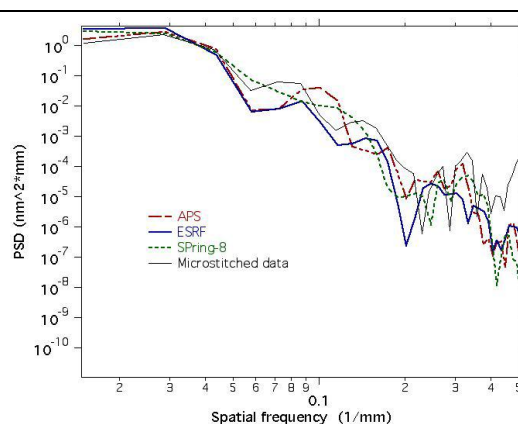
Figure 11: Results of the 100 mm Si substrate measurements: Power Spectral Density computed from the smoothed LTP

Proc. of SPIE 59210J-10

error data.	shape error profiles. Comparison is made with the PSD profile of microstitched data.

6. SUMMARY AND CONCLUSIONS

In this work we compared measurements of LTPs at three hard x-ray third-generation synchrotron radiation sources including the APS, the ESRF, and SPring-8. This was done by measuring selected mirrors that are representative of typical, as well as the state-of-the-art, mirrors currently used at these facilities. Despite significant differences in the LTP design and operation and in the metrology environment, the results were in remarkably good agreement. The maximum discrepancy of the rms slope error values is 0.1 µrad and that of the shape error is 3 nm, and they all relate to the measurement of the 1-m-long cylindrical mirror. The shortest mirror, fabricated by Osaka University, has a figure error (0.4 nm rms) beyond the LTP performance limits. The measured slope error profiles were dominated by noise. However, by the smoothing the data, it was still possible to extract the mirror surface slope and shape errors, and LTP results were independently confirmed by the microstitching interferometry measurements performed at Osaka University, thus giving confidence in the LTP data.

Uncertainties in the radii of curvature derived for the slope data could be explained by several possible sources of error: possible lack of consistency of mounting, a result of environment perturbations, or calibration. The largest discrepancy in the radius of curvature concerns the highly figured 100 mm silicon mirror. However, we note that this optic is nearly flat. Moreover, the radius of curvature calculation can be affected by a simple noise spike in the data. Also, remember this work is focused on flat mirrors. In general, mirrors with radii of curvature of a few tens of kilometers or larger are considered flat, and the mirror shape can be adjusted by a bending mechanism. The radius of curvature and shape become critical only when dealing with focusing mirrors used for obtaining a very small and optimized focused spot size, and this is particularly true for monolithic elliptical K-B mirrors. The next round-robin campaign will study elliptical and spherical optics, and it will provide the opportunity to tackle the radius of curvature measurements and calibration issues.

Finally, this collaborative work, along with a similar European round-robin measurement published in these proceedings [4], intend to set the basis for further work to evaluate and understand the limitations of the LTP and other similar profilers, develop guidelines and procedures to accurately perform measurements with them, and stimulate research to further improve their accuracy. A host of others issues were left for future work. These include, for example, a detailed study of measurement uncertainties of individual LTPs and a standard procedure to correct for systematic errors [14,16], which was only partially dealt with by mirror rotation and data averaging.

REFERENCES

1. P.Z. Takacs, S.N. Qian, and J. Colbert, "Design of a long trace surface profiler," Proc. SPIE **749** (1987) pp. 59-64.
2. P.Z. Takacs, S.N. Qian, Surface Profile Interferometer U.S. Patent No. 4,884,697 (1989).
3. S. Irick, " Long trace profiler survey," Proc. SPIE **3782** (1999) pp. 275-282.
4. Amparo Rommeveaux, Muriel Thomasset, Daniele Cocco, Frank Siewert, "First report on European round robin for slope measuring profilers," (*These proceedings*).
5. A. Khounsary, Argonne National Laboratory (*Private communication*).

6. Kazuto Yamauchi, Kazuya Yamamura, Hidekazu Mimura, Yasuhisa Sano, Akira Saito, Katsuyoshi Endo, Alexei Souvorov, Makina Yabashi, Kenji Tamasaku, Tetsuya Ishikawa, and Yuzo Mori, Jpn. J. Appl. Phys. **42** (2003) pp. 7129-7134.

7. Kazuto Yamauchi, Kazuya Yamamura, Hidekazu Mimura, Yasuhisa Sano, Akira Saito, Kazumasa Ueno, Katsuyoshi Endo, Alexi Souvorov, Makina Yabashi, Kenji Tamasaku, Tetsuya Ishikawa, and Yuzo Mori, Rev. Sci. Instrum. **74** (2003) pp. 2894-2898.

8. K. Von Bieren, "Pencil beam interferometer for aspherical optical surfaces laser diagnostics," Proc. SPIE 343 (1982).

9. Continental Optical Corp. 15 Power Drive, Hauppauge, NY 11788, USA. (Acquired by Ocean Optics, 830 Douglas Ave. Dunedin, FL 34698, USA).

10. Peter Z. Takacs, Eugene L. Church, Cynthia Bresloff, and Lahsen Assoufid, "Long Trace Profiler Measurement Repeatability Improvements," Appl. Optics **38** (1999), pp. 5468-5479.

11. Jean Susini, Robert Baker, Amparo Vivo, Optical Metrology Facility at the ESRF, Rev. of Sci. Instrum. **66** (1995) pp. 2232-2234.

12. Olivier Hignette, Amparo Rommeveaux, Status of the optical metrology at the ESRF, Proc. SPIE **2856** (1996) pp. 314-322.

13. S. Qian, W. Jark and P.Z. Takacs, Rev. Sci. Instrum. **66** (1995) pp. 2562-2569.

14. S. Irick,"Error reduction techniques for measuring long synchrotron mirrors," Proc. SPIE **3447** (1998) p 101.

15. E.L. Church and P.Z. Takacs, "BASIC Program for Power Spectrum Estimation," BNL report #49035 rev. 5/94.

16. Shinan Qian, Giovani Sostero, and Peter Z. Takacs,"Precision calibration and systematic error reduction in the long trace profiler," Optical Eng. **39** (2000) pp. 304-310.